Exploration of the energy dependence of proton nonlocal optical potentials

M. I. Jaghoub, A. E. Lovell, and F. M. Nunes

Exploration of the energy dependence of proton non-local optical potentials

M. I. Jaghoub,[1,2] A. E. Lovell,[1,3,4,5] and F. M. Nunes[1,3,*]

[1]*National Superconducting Cyclotron Laboratory, Michigan State University, East Lansing, MI 48824*
[2]*Physics Department, The University of Jordan, 11942 Amman, Jordan*
[3]*Department of Physics and Astronomy, Michigan State University, East Lansing, MI 48824-1321*
[4]*Theoretical Division, Los Alamos National Laboratory, Los Alamos, NM 87545*
[5]*Center for Nonlinear Studies, Los Alamos National Laboratory, Los Alamos, NM 87545*
(Dated: July 20, 2018)

Background: Given the importance of including nonlocality in the effective interactions in reaction models, a recent phenomenological study focusing on neutron-target non-local optical potentials suggests the need for the inclusion of explicit energy dependence (Phys. Rev. C 96, 051601).

Purpose: In this work, we inspect whether the same is true for proton non-local optical potentials.

Method: Similarly to the earlier work (Phys. Rev. C 96, 051601), we perform a χ^2 analysis of proton elastic scattering data on ^{40}Ca, ^{90}Zr and ^{208}Pb at energies ranging $E \approx 10 - 45$ MeV, assuming the Tian, Pang, and Ma non-local form for the optical potential. We introduce energy and asymmetry dependencies in the imaginary part of the potential and refit the data to obtain a global parameterization.

Results: No matter which starting point is used, or whether we include backward angles in the fitting procedure, our results show the emergence of a strong energy dependence in the potential. We also show that while our parameterization represents only a modest improvement over the original energy-independent potential for those cases included in the fit, our new energy-dependent potential extrapolates much better for nuclei not included in the fit and for energies above those included.

Conclusions: As for the neutron case, we conclude that non-locality alone cannot provide a complete description of proton elastic scattering data and that a significant energy dependence is required.

I. INTRODUCTION

Reactions with rare isotope beams have revived an important discussion on the best form to describe the effective interaction between a nucleon and a complex many-body nucleus. From the many-body formulation of the problem it is understood that the effective nucleon-target potential should be nonlocal but the form of the nonlocality may differ significantly based on the physics it is representing [1–3].

From earlier works (e.g. [4, 5]) to the recent times (e.g. [6]), understanding the correct form of the non-locality in the optical potential has been a focus of many studies. As discussed in [6], there are two main types of nonlocality in the optical potential. The first arises from antisymmetrization effects, can be described by a Gaussian shape, and is short range. The second is caused by channel coupling, can have a very different shape, and typically has a larger range. Recent optical potential studies based on the dispersive relation [7] are consistent with the existence of these two types of nonlocality. Whatever the type of nonlocality, the community has attempted to express the non-local character of the optical potential into simpler forms, such as a velocity dependence (e.g. [5, 8, 9]). Moreover, one must acknowledge that a large part of the reaction community still uses the traditional local energy-dependent optical potential, assuming that the energy dependence alone can make up for the effects of non-locality (e.g. [10, 11]). Even if a given set of elastic scattering data can usually be well described by a local approximation, studies in the last few years have revealed that the explicit inclusion of non-locality in the optical potential is important for other reaction channels and should be explicitly included [12–18].

In principle, one may be able to use microscopic calculations to derive the form of the optical potential. An example of such studies is the microscopic proton optical potentials based on the g matrix approach [19, 20] which provide good predictions for several reaction observables. However, more recent ab initio efforts [21, 22] demonstrate the difficulties of computing the optical potential from first principles, both due to model space truncations as well as deficiencies in the NN force. In this study, we focus on a phenomenological approach to proton optical potential and we limit the energy range to 10-65 MeV. This work follows an similar study for neutrons Ref.[23] where a broader introduction to the topic can be found.

The pioneering work of Perey and Buck (PB) [4] demonstrated that just by fitting neutron elastic scattering on ^{208}Pb at 7.0 and 14.5 MeV, one was able to obtain a parameterization that provided a good description of neutron elastic scattering across the nuclear chart. The form for the non-locality incorporated in the Perey and Buck parameterization is Gaussian which, as mentioned

earlier, accounts for antisymmetrization effects [4]. More recently Tian, Pang and Ma (TPM) [24] expanded that study to both neutron and proton scattering on a wider variety of targets. The fitting protocol for TPM included proton elastic scattering data on ^{27}Al, ^{56}Fe, ^{90}Zr, and ^{208}Pb at energies in the range $E = 16 - 30$ MeV. In both these efforts, the nonlocal parameterization is energy independent.

Optical potentials are known to be target dependent and contain an imaginary component, but as mentioned earlier, from a formal point of view, one also expects it to contain, both nonlocality and energy dependence [1–3, 25]. The question one should ask, given the importance of nonlocality in the interaction, is if the level of description in [4] and [24] is sufficient, or whether elastic scattering data calls for an explicit energy dependence in addition to the explicit non-locality. Lovell *et al.* [23] investigated this aspect for neutron-nucleus scattering. Starting from either PB or TPM, including a diverse set of spherical target nuclei as well as a couple of different angular cuts on the data, it was found that neutron elastic scattering data always prefers an explicit energy dependence in the interaction. In this work, we address the same question but now for proton elastic scattering.

The paper is organized as follows. In Section II we discuss the data, the general philosophy of the fitting procedure and some numerical details. The results are presented in Section III, followed by the conclusions in Section IV.

II. DATA AND FITTING PROCEDURE

In this work we focus on proton optical potentials to describe the scattering off of stable spherical nuclei. Just as in [23] we attempt to find the best description of the data with the minimum complexity. As for the neutron study [23] we include three targets in our fitting protocol, namely ^{40}Ca, ^{90}Zr and ^{208}Pb, so that the whole mass range is spanned. Data for these targets is abundant, and typically measured with large angular coverage. For each of these targets, we include angular distributions for five beam energies in the range $E = 10 - 45$ MeV. Specifically we include proton elastic scattering data on: ^{40}Ca at $E = 12.4, 16.0, 26.3, 30.0, 40.0$ MeV [26, 27]; ^{90}Zr at $E = 9.0, 12.7, 22.5, 30.0, 40.0$ MeV [28–32]; and ^{208}Pb at $E = 16.0, 24.1, 30.3, 35.0, 45.0$ MeV [33, 34]. As for [23], an overall error of 10% was included in the χ^2 minimization, based on the assumption that systematic errors in the cross section measurements outweigh the statistical errors typically included in the experimental papers.

We used NLAT [35] combined with sfresco [36] to perform χ^2 (per degree of freedom) minimizations for the angular distributions generated with the single-channel optical model assuming non-local potentials. We obtain 95% confidence bands by pulling parameters sets from the standard uncorrelated χ^2 distribution [37]. We also

compute, for each set of differential angular distributions (corresponding to a given target and beam energy), the χ^2 per degree of freedom. As in other fitting procedures (e.g. [38]), we can then group specific reactions by target or energy, summing the corresponding χ^2 per data set and dividing by the number of data sets included - here denoted χ^2_{set}. These χ^2_{set} are used to assess the quality of the results for the various targets and energy ranges.

The TPM proton potential [24], after partial wave decomposition, includes a real volume part and an imaginary volume part of the form:

$$g_\ell(r, r') = \frac{2i^\ell z}{\pi^{\frac{1}{2}}\beta} j_\ell(-iz) \exp\left(-\frac{r^2 + r'^2}{\beta^2}\right) U_{WS}\left(\frac{1}{2}(r + r')\right),$$
$$(1)$$

with r being the distance between the nucleon and the target. The potential U_{WS} is the standard Woods-Saxon form with the following parameters for the depth, radius and difuseness: $V = 70.95$ MeV, $r_v = 1.290$ fm, $a_v = 0.580$ fm for the real term and $W_i = 9.03$ MeV, $r_i = 1.240$ fm, $a_i = 0.5$ fm for the imaginary term. It also includes an imaginary surface term in which U_{WS} is replaced by the derivative of the Woods-Saxon with parameters: $W_s = 15.74$, $r_s = 1.20$ fm, $a_s = 0.45$ fm. The Gaussian nonlocality has range of $\beta = 0.88$ fm. In addition to the nonlocal potential, there are two terms that are local, namely the spin-orbit term (with parameters $V_{so} = 8.130$ MeV, $r_{so} = 1.020$ fm, $a_{so} = 0.590$ fm) and the regularized Coulomb term with Coulomb radius $r_c = 1.340$ fm. In this work we fix the local terms and the geometry of the nonlocal part of the interaction, and vary the potential depths V, W_i, W_s simultaneously.

As a first exploration, we fit each angular distribution individually using TPM as a starting point and obtain new V, W_i and W_s. We then analyze the dependence of these parameters with mass number A and beam energy E. For the real depth V we found that no energy dependence was needed but the data did require a weak mass dependence:

$$V = 67.047 + 0.0238A. \qquad (2)$$

Here the parameter V has units of MeV. Note that this was not necessary for the neutron scattering case [23]. The imaginary depths coming from fitting the proton elastic scattering data showed a strong variation with both mass and beam energy, a dependence that could be described approximately as linear, similarly to other global potentials (e.g. [38]).

We then consider a form for the mass and energy dependence similar to [23]:

$$W_i = a_v^E E + a_v^{asym} (N - Z)/A + a_v^0,$$
$$W_s = a_s^E E + a_s^{asym} (N - Z)/A + a_s^0, \qquad (3)$$

where the depths (W_i and W_s) and the energy (E) are provided in units of MeV. Using the dependence in Eqs.(2) and (3) and all 15 data sets simultaneously, we perform a six parameter fit (for

$\theta < 100°$	a_v^E	a_v^{asym} (MeV)	a_v^0 (MeV)	a_s^E	a_s^{asym} (MeV)	a_s^0 (MeV)
neutron [23]	0.02 ± 0.009	$(fixed)0$	0.36 ± 0.26	0.20 ± 0.004	4.50 ± 0.50	12.15 ± 0.40
neutron (TPM)	0.23 ± 0.006	$(fixed)0$	-0.75 ± 0.10	0.12 ± 0.005	5.33 ± 0.59	13.92 ± 0.22
TPM-E	0.03 ± 0.014	51.14 ± 3.22	0.405 ± 0.38	0.18 ± 0.011	9.08 ± 3.79	11.16 ± 0.37
TPM-E0	$(fixed)\ 0$	49.19 ± 3.19	1.86 ± 0.36	0.23 ± 0.015	9.72 ± 3.79	9.07 ± 0.62
MJ-E	-0.17 ± 0.015	45.75 ± 3.51	7.86 ± 0.23	0.42 ± 0.011	11.86 ± 3.88	2.47 ± 0.36

TABLE I: Best fit parameters using TPM as starting point for the minimization, fitting data with $\theta < 100°$.

$\theta \leq 180°$	a_v^E	a_v^{asym} (MeV)	a_v^0 (MeV)	a_s^E	a_s^{asym} (MeV)	a_s^0 (MeV)
TPM-E	0.14 ± 0.004	23.21 ± 0.50	4.62 ± 0.09	0.73 ± 0.003	-5.09 ± 0.10	14.43 ± 0.66
MJ-E	0.306 ± 0.008	32.33 ± 0.79	0.20 ± 0.01	0.578 ± 0.005	-0.79 ± 0.047	7.47 ± 0.34

TABLE II: Best fit parameters using TPM as starting point for the minimization, fitting the full range of data $\theta \leq 180°$.

$a_v^E, a_v^{asym}, a_v^0, a_s^E, a_s^{asym}, a_s^0$) starting from the original TPM potential. We estimate the errors on the parameters directly from the covariance matrix.

III. RESULTS

Tables I and II summarize the results of our fitting procedure. The first row in Table I corresponds to the parameterization obtained in [23] for the neutrons, when the regression based on independent fits is taken as a starting point, and only data up to 100° are included (labeled in [23] as TPM-E). We also show the results for the neutron potential when the neutron TPM potential is taken as a starting point (second row) and the fitting procedure included the same neutron data as in Ref. [23]. This fit was performed recently for the sake of comparison with the proton results. These two sets of parameters for neutrons demonstrate immediately that the parameters depend strongly on the initial point, but in both cases a strong energy dependence is obtained as in Ref. [23].

The parameters obtained for the proton interaction, for identical conditions (here denoted by TPM-E), are shown in the third row. Apart from the asymmetry terms, a_v^{asym} and a_s^{asym}, the parameters obtained for neutrons and protons are similar, supporting the idea of charge symmetry and suggesting similar properties of the χ^2 function. The interaction obtained for the protons has a strong asymmetry dependence, with errors of 10% on the parameters a_v^{asym} and a_s^{asym}. The magnitude of the surface asymmetry term is similar to that obtained for the local parameterizations in [38], although in those earlier studies, no asymmetry dependence is included in the volume part of the imaginary potential.

Most importantly for this work, the energy dependence in the imaginary surface term a_s^E is significant, just as for the neutron case. Since a_v^E is very close to zero, one might ask whether the energy dependence in the volume part of the imaginary potential can be removed. Thus, we repeated the fitting process with $a_v^E = 0$. The resulting parameters are shown in the third row of Table I (TPM-

E0). These are very similar to the TPM-E parameters, but a_s^E increases to compensate for the lack of energy dependence in the volume part.

As for the neutrons, the proton parameterizations are strongly dependent on initialization. For the neutron cases presented in [23], fits to individual data sets were produced starting from either the Perey and Buck potential [4] or from TPM [24]. The linear regressions as a function of energy were then used to produce the full fits. These two starting points provided very different parameterizations.

The potential labeled here as TPM-E starts directly from TPM. Given that PB was only developed for neutrons, it would not make sense to use it as an initialization here. We thus performed regressions over energy and asymmetry for the parameters resulting from the individual fits, mimicking the dependences in Eq.3. That gave us a new starting point for the joint fit to all 15 sets of data. The resulting parameters are shown in the last row of Table I (MJ-E) and correspond to a very different minimum. While parameters are very different, there are two important aspects that remain unchanged: first there remains a significant energy dependence through a_s^E and second the asymmetry terms remain large. Note that the negative slope a_v^E is a cause for concern, given that it is likely to provide unreliable extrapolations to high energy. We will return to this point in Section III B.

As for [23], we investigate the differences obtained in the parameterizations when all the data is included (full angular range) and only angles up to $\theta < 100°$ are considered. Table II shows the resulting parameters including data for the full angular range in the fit, for a TPM initialization (TPM-E) or a initialization based on the independent fits (MJ-E). The resulting parameters change significantly from those shown in Table I, but the energy dependence in the imaginary surface term remains strong. The results show an interaction with a much stronger energy dependence, and an unexpected negative dependence in asymmetry. It is understood that the optical model will not perform well for backward angles where complex coupling processes are expected to
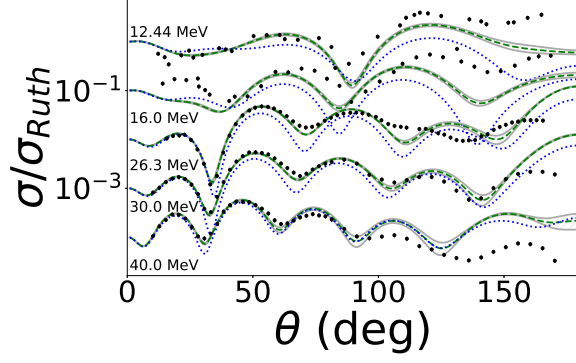
FIG. 1: (Color online) Angular distributions for ^{40}Ca$(p,p)^{40}$Ca at E = 12.4, 16, 26.3, 30, 40 MeV. Comparison of the predictions using TPM-E (green-dashed lines) with TPM (blue-dotted line) and the data [26, 27].
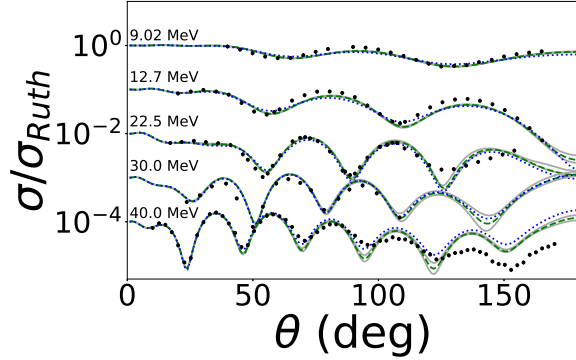

FIG. 2: (Color online) Angular distributions for ^{90}Zr$(p,p)^{90}$Zr at E = 9, 12.7, 22.5, 30, 40 MeV. Comparison of the predictions using TPM-E (green-dashed lines) with TPM (blue-dotted line) and the data [28–32].
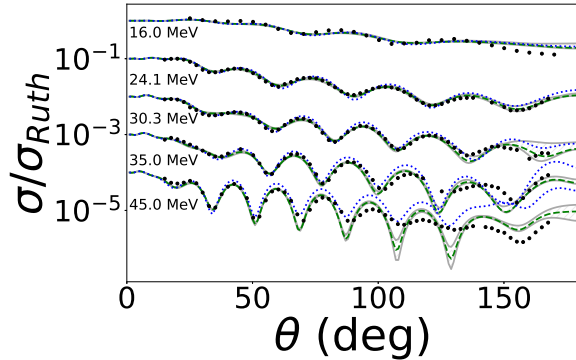

FIG. 3: (Color online) Angular distributions for ^{208}Pb$(n,n)^{208}$Pb at E = 16, 24.1, 30.3, 35, 45 MeV. Comparison of the predictions using TPM-E (green-dashed lines) with TPM (blue-dotted line) and the data [33, 34].

	TPM-E	TPM	MJ-E
^{40}Ca ($E \leq 45$ MeV)	72.0	70.2	69.1
^{90}Zr ($E \leq 45$ MeV)	20.6	48.5	20.0
^{208}Pb ($E \leq 45$ MeV)	8.6	117.1	8.5
Total ($E \leq 45$ MeV)	101.1	235.8	97.5
^{32}S ($E \leq 45$ MeV)	12.2	15.9	13.8
^{68}Zn ($E \leq 45$ MeV)	17.7	32.3	17.9
^{89}Y ($E \leq 45$ MeV)	9.73	10.9	12.3
^{100}Mo ($E \leq 45$ MeV)	23.2	30.8	24.3
^{110}Pd ($E \leq 45$ MeV)	31.8	44.3	30.0
Total ($E \leq 45$ MeV)	94.6	134.2	98.4
^{32}S ($45 < E \leq 65$ MeV)	400.9	826.5	313.8
^{68}Zn ($45 < E \leq 65$ MeV)	503.6	1437.3	482.6
^{89}Y ($45 < E \leq 65$ MeV)	48.2	82.9	53.9
^{100}Mo ($45 < E \leq 65$ MeV)	30.9	62.5	34.0
^{110}Pd ($45 < E \leq 65$ MeV)	235.2	718.9	203.0
Total ($45 < E \leq 65$ MeV)	1219	3128	1087

TABLE III: χ^2_{set} for proton elastic scattering on the various targets here considered: our energy parameterization TPM-E from Table I is shown in column 2 and compared with the original TPM in column 3 and MJ-E in column 4.

dominate. From here on, we focus on the fits obtained including data only up to 100°.

A. Results for fitted cases

We now turn to assessing the quality of the fits, in comparison to the original TPM interaction. In this section we first focus on the results obtained for those cases that were included in the fitting protocol, and then, in Section III B, we discuss the predictions for targets not included in the protocol and for energies outside the fitted range ($E > 45$ MeV).

The angular distributions obtained with TPM-E from Table I are shown in Figs. 1, 2, and 3 for proton elastic scattering off of ^{40}Ca, ^{90}Zr and ^{208}Pb, respectively (green dashed lines). Included in grey are the 95% confidence bands. For comparison, we also show the angular distributions obtained with the original TPM interaction (blue dotted lines). There are several cases for which TPM-E improves the description of the data over TPM. Visually, the data for ^{40}Ca at the lower energies is better described by TPM-E, as well as the ^{208}Pb data for the higher energies. Strikingly, TPM-E and TPM both do very well in describing the ^{90}Zr data across the energy range here considered. This is not surprising since the original TPM already included ^{90}Zr data in the fit.

In order to quantify the goodness of the fit, we show in Table III the χ^2, divided by the number of data sets, for the various targets considered. These χ^2 are computed for the whole angular range, even though TPM-E was determined from a fit including data only up to 100°. The

improvement obtained by including the energy dependence is significant for both ^{90}Zr and ^{208}Pb, but mostly due to the highest energy here considered (the original TPM potential was fit with elastic scattering data up to 30 MeV). For the ^{40}Ca case, the averaged χ^2 does not show a significant improvement although, as we saw for the angular distributions, there is a clear improvement at the lower energies. Even though ^{40}Ca was not explicitly included in the original TPM fit, TPM does very well in describing proton elastic scattering on ^{40}Ca for energies around 30 MeV.

Overall, the total χ^2 for TPM-E is significantly reduced compared to that obtained with TPM due to the χ^2 being calculated out to 180°. For completeness, we also include the resulting χ^2 values when angular distributions are computed with the interaction provided in the last row in Table I (MJ-E). Even though the parameterization is somewhat different, the resulting χ^2 are very close to those obtained with TPM-E. While the χ^2 is reduced by 133% from TPM to TPM-E, the difference between MJ-E and TPM-E is less than 5%.

The 95% confidence bands associated with TPM-E and shown in Figs. 1, 2, and 3 are rather narrow, especially considering the large errors on some of the parameters in the TPM-E fit. Results in [37] demonstrate that when an uncorrelated χ^2 function is used, the resulting confidence bands are unphysicaly narrow. One can expect that, if instead of using the standard uncorrelated χ^2 function we had used a correlated χ^2 function, these confidence bands would widen considerably.

Finally, we discuss the nonlocality range. In the early work of Perey and Buck [4], the nonlocality included in the interaction was Gaussian with a range based on the properties of the NN interaction ($\beta = 0.85$ fm). This was kept constant in their fit to elastic scattering data. The original TPM interaction was determined from a fit that included the nonlocality range as a fitting parameter ($\beta = 0.88$ fm). In our work, the nonlocality range β was fixed at the original TPM value, assuming this corresponded indeed to the minimum for proton elastic scattering. However, given that the energy dependence introduced in this work is significant, we felt it was necessary to explore the χ^2 function around this $\beta = 0.88$ fm value by refitting the parameters in Table I starting with either $\beta_0 = 0.2$ fm or with $\beta_0 = 1.0$ fm. We found that the minimum in the χ^2-function was obtained for β in the range $0.84 - 0.86$ fm, although the differences in the resulting χ^2 at the minima were so small that it did not justify the addition of one more free parameter in the fit; the χ^2-function is essentially flat with β around the TPM value. We thus kept the original TPM value of $\beta = 0.88$ fm throughout this work.

Given the different sources of nonlocality [6], this result is somewhat surprising. To account for channel coupling effects, one would expect the need for a larger range in the non-locality. However, this set of elastic data does not require such a description. This is likely due to the fact that the nuclei included in the fitting protocol are, to a good approximation, spherical, and their elastic scattering is fairly well described within a single-channel description. We do expect that, when focusing on light targets or nuclei further from stability, the nonlocality range would likely increase and one may need different terms in the interaction, with multiple nonlocality ranges as in [7].

B. Results for predicted cases

We now use TPM-E to make predictions of cross sections and test the quality of these predictions with existing data. For that purpose we consider proton elastic scattering on: ^{32}S at 15, 17.7, 19, 21, 23, 25, 65 MeV [39, 40]; ^{68}Zn at 20.4, 30.5, 39.6, 49, 61.4 MeV [41–44]; ^{89}Y at 21.1, 49.4, 65 MeV [45–47]; ^{100}Mo at 15, 30.3, 49.5, 65 MeV [48–50]; and ^{110}Pd at 22 and 52 MeV [51, 52].

Fig. 4 shows that angular distributions for proton elastic scattering on ^{68}Zn at 39.6 MeV and ^{100}Mo at 30 MeV. These cases correspond to interpolations of the TPM-E parameterization of Table I as a function of mass, asymmetry and beam energy. The green-dashed line is the prediction using TPM-E while the blue-dotted line represent the results using the original TPM interaction. The corresponding 95% confidence bands for TPM-E are also provided (gray bands). These results illustrate the modest improvement obtained when using the explicit energy dependence in the interaction for those cases within the fitted range.

Fig. 5 shows the predicted angular distributions for proton elastic scattering on ^{32}S, which is outside the fitted mass region. As before, the 95% confidence bands for TPM-E are shown in gray. The figure shows that the TPM-E interaction, which includes a small mass dependence on the real part of the potential, is able to provide a satisfactory description of elastic scattering, as opposed to TPM which does not perform well. This is despite the fact that the TPM fitting protocol does include light masses, namely ^{27}Al.

Finally in Fig. 6 we show predictions for proton elastic scattering angular distributions for a higher energy, outside the range where the interactions were fitted. Due to the explicit energy dependence introduced in TPM-E, this interaction performs better than the original energy independent TPM.

Table III includes the χ^2 for each of the data sets considered in testing the predictive power of TPM-E. For the 5 targets studied, we first only include beam energies within the range that was fitted. We see an improvement of TPM-E over TPM of the same magnitude as that obtain for the fitted cases (^{40}Ca, ^{90}Zr and ^{208}Pb). We then also show the resulting χ^2 per data set, obtained when including the higher energies up to 65 MeV. Expectedly, in this case the improvement is much larger. However, in some cases, the resulting χ^2 using TPM-E is still very large, which suggests that the linear energy dependence may already break down for energies $E > 50$ MeV. This
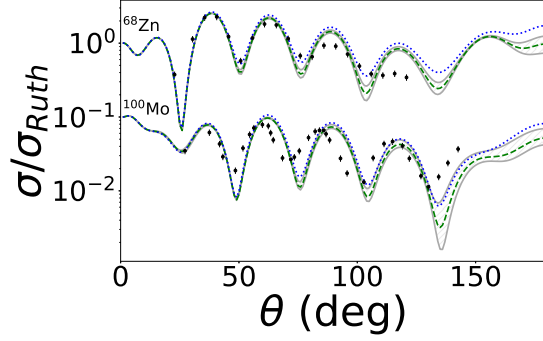
FIG. 4: (Color online) Angular distributions for proton elastic scattering for targets within the fitted mass range $A = 40 - 208$ and at an energy within $E = 9 - 45$ MeV. Comparison of the predictions using TPM-E (green-dashed lines) with TPM (blue-dotted line) and the data [43, 49].
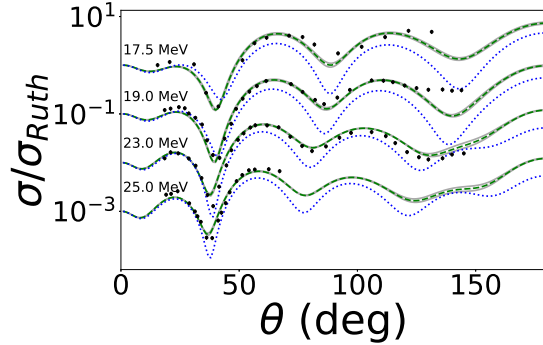

FIG. 5: (Color online) Angular distributions for $^{32}\mathrm{S}(p,p)^{32}\mathrm{S}$ at $E = 17.5, 19, 23, 25$ MeV. Comparison of the predictions using TPM-E (green-dashed lines) with TPM (blue-dotted line) and the data [39].
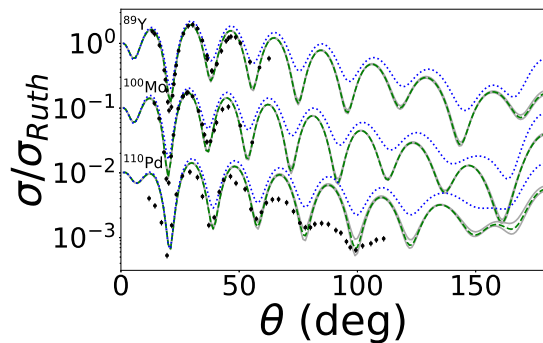

FIG. 6: (Color online) Angular distributions for proton elastic scattering on $^{89}\mathrm{Y}$, $^{100}\mathrm{Mo}$ and $^{110}\mathrm{Pd}$ at beam energies outside the fitted range, namely 65 MeV for the two first cases and 52 MeV for the last. Comparison of the predictions using TPM-E (green-dashed lines) with TPM (blue-dotted line) and the data [47, 50, 52].

is a known problem with phenomenological approaches (e.g. [11]), a problem that can be reduced by using the dispersion relation to further constrain the interaction [53].

In Table III we also show the χ^2 values obtained when using the MJ-E parameterization. As for the fitted cases, MJ-E provides very similar χ^2 as the TPM-E parameterization. The difference of roughly 5% is not significant compared to the large improvement over the original TPM interaction. Also, it appears that the negative slope a_v^E does not cause problems up to $E = 65$ MeV.

Finally, we need to consider the asymmetry term in this interaction. First of all, contrary to the neutron case, we found it necessary to include an asymmetry dependence in the imaginary volume part of the interaction. This resulted in a very large a_v^{asym} parameter, regardless of the starting point. Such a large asymmetry dependence in the volume imaginary term of the optical potential is not observed for local potentials. In addition, the asymmetry dependence of the surface imaginary potential a_s^{asym} doubled compared to the values obtained for the neutron elastic scattering study [23]. As mentioned before, its numerical value is very much in line with that of a local parameterization of [38]. Moreover, if the proton elastic scattering fit includes data in the full angular range, the asymmetry dependence is much reduced and even changes sign for the surface asymmetry. This will result on a cancellation of the effect of the imaginary volume term.

Note that the energy range over which the TPM predictions deviate largely from the experimental data is not the same for proton-target and neutron-target interactions. For neutrons, energy dependence was required above 40 MeV, while for the protons, the transition occured around 50 MeV. This difference is likely due to the Coulomb repulsion.

All nuclei for which we made predictions have asymmetries within the range of asymmetries included in the fit $\frac{N-Z}{A} = 0 - 0.21$. It is thus evident that the interpolations provided by the asymmetry dependence we obtain, are reliable. However, it is unclear how the asymmetry dependence of the parameterizations of Table I will extrapolate outside the region, and in particular when moving away from stability into the neutron-rich and proton-rich regions of the nuclear chart.

Based on physics considerations, one might assume the asymmetry coefficient for the neutron and proton to be of the same magnitude but opposite sign. We have thus rerun the neutron case of Ref. [23], fixing the asymmetries $a_v^{asym} = -51.14$ MeV and $a_s^{asym} = -9.080$ MeV. The resulting minimum has a much larger χ^2 value (4 times worse). The resulting parameterization has a much stronger energy dependence in the volume term, while the surface term suffers only a modest modification: $a_s^E = 0.453$; $a_s^0 = 21.17$ MeV ; $a_v^E = 0.26$; and $a_v^0 = 18.77$ MeV. Further work is needed to better understand the asymmetry dependence of a nonlocal global potential and the inter-relation between neutron and pro-

ton parameters.

IV. CONCLUSIONS

Following the study of energy dependence of nonlocal optical potentials for neutron elastic scattering [23], in this work, we look into the energy dependence of proton elastic scattering. Namely, we want to answer the question of whether the inclusion of an explicit Gaussian nonlocality can fully account for the complexity of the effective proton-nucleus interaction, or whether the elastic data calls for an additional energy dependence in the interaction.

With this goal in mind, we performed a joint fit to proton elastic scattering data for a range of energies $E = 10 - 45$ MeV on ^{40}Ca, ^{90}Zr and ^{208}Pb. We use the energy independent nonlocal parameterization of Ref.[24] as our starting point. Motivated by local global parameterizations and by the fits to the individual elastic scattering data, we introduce a linear energy dependence on both the surface and volume imaginary parts of the interaction, as well as asymmetry terms.

Our results show that this energy dependent nonlocal interaction (TPM-E) offers a modest improvement over the original TPM for those cases in our fitting protocol. However, TPM-E presents a larger improvement over TPM for those nuclei with masses outside the range included in the fit, as well as for extrapolations in energy up to $E = 65$ MeV. We also show that although the details of the parameterization obtained does depend on the initial starting point for the fitting protocol, the magnitude of the energy dependent component is identical and the resulting quality of the fit is similar for the two different initializations considered here (TPM-E and MJ-E). Finally, we also confirm that our conclusions concerning the energy dependence do not change when the nonlocality range parameter is allowed to vary in the fit.

In addition to the energy dependence, our study gives rise to a large asymmetry dependence in the optical potential. Although the errors on a_v^{asym} and a_s^{asym} are small, of the order of 10%, we do not believe the asymmetry dependence is robust. Most importantly, when comparing with the neutron case [23], we do not understand the physical reason for its emergence.

This study confirms that the Gaussian nonlocality introduced explicitly in the optical potential is not sufficient to properly describe proton elastic scattering. This result is consistent with [6, 23], and justifies a more comprehensive study to extract a new energy dependent nucleon-nucleus non-local optical potential. This study should also consider cases away from stability to become useful for research on rare isotope worldwide.

[1] H. Feshbach, Ann. Phys. **5**, 357 (1958), ISSN 0003-4916.

[2] H. Feshbach, Ann. Phys. **19**, 287 (1962), ISSN 0003-4916.

[3] W. Dickhoff and D. Van Neck, *Many-Body Theory Exposed! 2nd ed.* (World Scientific, New Jersey, 2008).

[4] F. Perey and B. Buck, Nucl. Phys. **32**, 353 (1962), ISSN 0029-5582.

[5] L. G. Arnold, Phys. Rev. Lett. **26**, 1263 (1971), URL https://link.aps.org/doi/10.1103/PhysRevLett.26.1263.

[6] Fraser, P., Amos, K., Karataglidis, S., Canton, L., Pisent, G., and Svenne, J. P., Eur. Phys. J. A **35**, 69 (2008), URL https://doi.org/10.1140/epja/i2007-10524-1.

[7] M. H. Mahzoon, R. J. Charity, W. H. Dickhoff, H. Dussan, and S. J. Waldecker, Phys. Rev. Lett. **112**, 162503 (2014).

[8] G. H. Rawitscher and D. Lukaszek, Phys. Rev. C **69**, 044608 (2004), URL https://link.aps.org/doi/10.1103/PhysRevC.69.044608.

[9] M. I. Jaghoub, M. F. Hassan, and G. H. Rawitscher, Phys. Rev. C **84**, 034618 (2011), URL https://link.aps.org/doi/10.1103/PhysRevC.84.034618.

[10] R. Varner, W. Thompson, T. McAbee, E. Ludwig, and T. Clegg, Phys. Rep. **201**, 57 (1991), ISSN 0370-1573.

[11] A. Koning and J. Delaroche, Nucl.Phys. **A713**, 231 (2003).

[12] L. J. Titus and F. M. Nunes, Phys. Rev. C **89**, 034609 (2014).

[13] A. Ross, L. J. Titus, F. M. Nunes, M. H. Mahzoon, W. H. Dickhoff, and R. J. Charity, Phys. Rev. C **92**, 044607 (2015), URL http://link.aps.org/doi/10.1103/PhysRevC.92.044607.

[14] L. J. Titus, F. M. Nunes, and G. Potel, Phys. Rev. C **93**, 014604 (2016), URL http://link.aps.org/doi/10.1103/PhysRevC.93.014604.

[15] A. Ross, L. J. Titus, and F. M. Nunes, Phys. Rev. C **94**, 014607 (2016), URL http://link.aps.org/doi/10.1103/PhysRevC.94.014607.

[16] N. K. Timofeyuk and R. C. Johnson, Phys. Rev. C **87**, 064610 (2013).

[17] S. J. Waldecker and N. K. Timofeyuk, Phys. Rev. C **94**, 034609 (2016), URL http://link.aps.org/doi/10.1103/PhysRevC.94.034609.

[18] G. W. Bailey, N. K. Timofeyuk, and J. A. Tostevin, Phys.

Rev. Lett. **117**, 162502 (2016), URL http://link.aps.org/doi/10.1103/PhysRevLett.117.162502.

[19] P. J. Dortmans, K. Amos, S. Karataglidis, and J. Raynal, Phys. Rev. C **58**, 2249 (1998), URL https://link.aps.org/doi/10.1103/PhysRevC.58.2249.

[20] P. K. Deb, K. Amos, and S. Karataglidis, Phys. Rev. C **62**, 037601 (2000), URL https://link.aps.org/doi/10.1103/PhysRevC.62.037601.

[21] J. Rotureau, P. Danielewicz, G. Hagen, F. M. Nunes, and T. Papenbrock, Phys. Rev. C **95**, 024315 (2017), URL http://link.aps.org/doi/10.1103/PhysRevC.95.024315.

[22] A. Kumar, R. Kanungo, A. Calci, P. Navrátil, A. Sanetullaev, M. Alcorta, V. Bildstein, G. Christian, B. Davids, J. Dohet-Eraly, et al., Phys. Rev. Lett. **118**, 262502 (2017), URL https://link.aps.org/doi/10.1103/PhysRevLett.118.262502.

[23] A. E. Lovell, P.-L. Bacq, P. Capel, F. M. Nunes, and L. J. Titus, Phys. Rev. C **96**, 051601 (2017), URL https://link.aps.org/doi/10.1103/PhysRevC.96.051601.

[24] Y. Tian, D.-Y. Pang, and Z.-Y. Ma, Int. J. Mod. Phys. E **24**, 1550006 (2015).

[25] K. Amos, P. J. Dortmans, H. V. von Geramb, S. Karataglidis, and J. Raynnal, *Nucleon-Nucleus Scattering: A Microscopic Nonrelativistic Approach* (Springer US, Boston, MA, 2002), pp. 276–536, ISBN 978-0-306-47101-8, URL https://doi.org/10.1007/0-306-47101-9_3.

[26] J. F. Dicello, G. Igo, W. T. Leland, and F. G. Perey, Phys. Rev. C **4**, 1130 (1971), URL https://link.aps.org/doi/10.1103/PhysRevC.4.1130.

[27] R. H. McCamis, T. N. Nasr, J. Birchall, N. E. Davison, W. T. H. van Oers, P. J. T. Verheijen, R. F. Carlson, A. J. Cox, B. C. Clark, E. D. Cooper, et al., Phys. Rev. C **33**, 1624 (1986), URL https://link.aps.org/doi/10.1103/PhysRevC.33.1624.

[28] N. A.F.Gurbich, Vop. At.Nauki i Tekhn.,Ser.Yadernye Konstanty **1996**, 142 (1996).

[29] J. K. Dickens, E. Eichler, and G. R. Satchler, Phys. Rev. **168**, 1355 (1968), URL https://link.aps.org/doi/10.1103/PhysRev.168.1355.

[30] J. B. Ball, C. B. Fulmer, and R. H. Bassel, Phys. Rev. **135**, B706 (1964), URL https://link.aps.org/doi/10.1103/PhysRev.135.B706.

[31] G. R.De Swiniarski, Dinh-Lien Pham, Canadian Journal of Physics **55**, 43 (1977).

[32] L. N. Blumberg, E. E. Gross, A. VAN DER Woude, A. Zucker, and R. H. Bassel, Phys. Rev. **147**, 812 (1966), URL https://link.aps.org/doi/10.1103/PhysRev.147.812.

[33] R.Varner, Thesis (1986).

[34] W. T. H. van Oers, H. Haw, N. E. Davison, A. Ingemarsson, B. Fagerström, and G. Tibell, Phys. Rev. C **10**, 307 (1974), URL https://link.aps.org/doi/10.1103/PhysRevC.10.307.

[35] L. Titus, A. Ross, and F. Nunes, Comput. Phys. Commun. **207**, 499 (2016), ISSN 0010-4655, URL http://www.sciencedirect.com/science/article/pii/S0010465516302028.

[36] I. J. Thompson, Comput. Phys. Rept. **7**, 167 (1988).

[37] A. E. Lovell, F. M. Nunes, J. Sarich, and S. M. Wild, Phys. Rev. C **95**, 024611 (2017), URL https://link.aps.org/doi/10.1103/PhysRevC.95.024611.

[38] J. Becchetti, F.D. and G. Greenlees, Phys. Rev. **182**, 1190 (1969).

[39] W. T. H. van Oers, H. Haw, N. E. Davison, A. Ingemarsson, B. Fagerström, and G. Tibell, Phys. Rev. C **10**, 307 (1974), URL https://link.aps.org/doi/10.1103/PhysRevC.10.307.

[40] S. Kato, K. Okada, M. Kondo, K. Hosono, T. Saito, N. Matsuoka, K. Hatanaka, T. Noro, S. Nagamachi, H. Shimizu, et al., Phys. Rev. C **31**, 1616 (1985), URL https://link.aps.org/doi/10.1103/PhysRevC.31.1616.

[41] W. H. L. Moonen, J. H. A. M. Krabbenborg, H. P. Offermans, J. F. A. G. Ruyl, P. J. van Hall, S. S. Klein, G. J. Nijgh, C. W. A. M. van Overveld, R. M. A. L. Petit, and O. J. Poppema, Journal of Physics G: Nuclear and Particle Physics **19**, 1191 (1993), URL http://stacks.iop.org/0954-3899/19/i=8/a=009.

[42] W. Tait, E. Burge, and V. Edwards, Nuclear Physics A **176**, 390 (1971), ISSN 0375-9474, URL http://www.sciencedirect.com/science/article/pii/0375947471902776.

[43] H. S. Liers, R. N. Boyd, C. H. Poppe, J. A. Sievers, and D. L. Watson, Phys. Rev. C **2**, 1399 (1970), URL https://link.aps.org/doi/10.1103/PhysRevC.2.1399.

[44] C. B. Fulmer, J. B. Ball, A. Scott, and M. L. Whiten, Phys. Rev. **181**, 1565 (1969), URL https://link.aps.org/doi/10.1103/PhysRev.181.1565.

[45] J. Melssen, P. V. Hall, S. Wassenaar, O. Poppema, G. Nijgh, and S. Klein, Nuclear Physics A **376**, 183 (1982), ISSN 0375-9474, URL http://www.sciencedirect.com/science/article/pii/0375947482900598.

[46] G. Mani, D. Jones, and D. Jacques, Nuclear Physics A **165**, 384 (1971), ISSN 0375-9474, URL http://www.sciencedirect.com/science/article/pii/0375947471907664.

[47] H. Sakaguchi, M. Nakamura, K. Hatanaka, A. Goto, T. Noro, F. Ohtani, H. Sakamoto, and S. Kobayashi, Physics Letters B **89**, 40 (1979), ISSN 0370-2693, URL http://www.sciencedirect.com/science/article/pii/0370269379900716.

[48] H. F. Lutz, D. W. Heikkinen, and W. Bartolini, Phys. Rev. C **4**, 934 (1971), URL https://link.aps.org/doi/10.1103/PhysRevC.4.934.

[49] B. Sinha, V. Edwards, E. Burge, and W. Tait, Nuclear Physics A **183**, 401 (1972), ISSN 0375-9474, URL http://www.sciencedirect.com/science/article/pii/0375947472906677.

[50] H. Sakaguchi, M. Nakamura, K. Hatanaka, A. Goto, T. Noro, F. Ohtani, H. Sakamoto, H. Ogawa, and S. Kobayashi, Phys. Rev. C **26**, 944 (1982), URL https://link.aps.org/doi/10.1103/PhysRevC.26.944.

[51] Y. Aoki, H. Iida, K. Hashimoto, K. Nagano, M. Takei, Y. Toba, and K. Yagi, Nuclear Physics A **394**, 413 (1983), ISSN 0375-9474, URL http://www.sciencedirect.com/science/article/pii/037594748390115X.

[52] M. Koike, T. Suehiro, K. Pingel, K. Komura, I. Nonaka, T. Wada, T. Fujisawa, H. Kamitsubo, and T. Nojiri, Nuclear Physics A **248**, 237 (1975), ISSN 0375-9474, URL http://www.sciencedirect.com/science/article/pii/0375947475901645.

[53] C. Mahaux and R. Sartor, in *Advances in Nuclear Physics*, edited by J. Negele and E. Vogt (Springer US, 1991), vol. 20 of *Advances in Nuclear Physics*, pp. 1–223, ISBN 978-1-4613-9912-4, URL http://dx.doi.org/10.